PROCEEDINGS. Twenty-second Workshop **on** Geothermal Reservoir Engineering
Stanford University, Stanford, California, **January** 27-29, **1997**
SGP-TR-155

HYDROTHERMAL ALTERATION AND FLUID-INCLUSION SYSTEMATICS OF THE RESERVOIR ROCKS IN MATALIBONG-25, TIWI, PHILIPPINES

Joseph N. Moore[1], Thomas **S.** Powell[2], David I. Norman[3] and Glenn W. Johnson[1]

1. Energy and Geoscience Institute, University of Utah, Salt Lake City, UT 84108
2. Unocal Geothermal and Power Operations, Santa Rosa CA 95401
3. Dept. of Geosciences, New Mexico Tech, Socorro NM 87801

ABSTRACT

The Tiwi geothermal field is related to young volcanic activity on the southern part of Luzon Island, Philippines. In 1992, nearly 1650 m of continuous core was obtained from the western part of the Matalibong sector where measured temperatures are close to 270°C.

Eight stages of alteration and vein mineralization have been documented. The earliest stage is characterized by phyllic alteration of the reservoir rocks (stage 1). Stages 2 through 6 produced veins characterized by quartz + epidote + pyrite (stage 2), anhydrite + calcite (stage 3), epidote and/or quartz and/or adularia (stage 4), calcite + anhydrite (stage 5), wairakite and/or epidote + quartz (stage 6), calcite (stage 7), and illite ±chlorite (stage **8).** The maximum fluid-inclusion temperatures of stages 3, 4, and **5** vein minerals are close to the boiling point and typically exceed 300°C while minimum temperatures are as much as 35°C below the present measured temperatures. Together, these data lead to the conclusion that mineralization reflects: 1) early heating of the system (stage 1); 2) successive periods of boiling, pressure drawdown and the incursion of cooler fluids (stages 2-3; 4-5; 6-7); and *3)* renewed heating and boiling (stage 8) in response to the emplacement of recent intrusions beneath Mt. Malinao.

$^{40}Ar/^{39}Ar$ spectrum dating of adularia from a stage 4 quartz-adularia-sulphide cemented breccia has yielded a minimum age of 0.32 Ma for adularia deposition and indicates that temperatures were higher than 275°C between 0.32 and 0.25 Ma. When these data are combined with fluid inclusion and mineral geothermometers, they constrain the ages of stages 1-7 to more than 0.25 Ma. Fluid-mineral modeling indicates that the youngest stage of mineralization (stage 8 sericite) is in equilibrium with the present-day fluids (Bruton et al., 1997).

Fluid-inclusion salinities suggest that the mineralizing fluids below a depth of 1600 m were dominated by seawater whereas the fluids at shallower depths were dominantly fresh waters. Gases contained in the inclusions are characterized by significant contents of CO_2, CH_4, N_2, Ar, and locally H_2S. The data suggest that the original meteoric signature of the gases has been modified by gases derived from crustal and possibly magmatic sources. Possible contributions of magmatic gases are indicated by high N_2/Ar ratios.

INTRODUCTION

The Tiwi geothermal field, with an installed capacity of 330 MWe, is a major producer of electricity in the Philippines (Gambill and Beraquit, 1993). Although development of the field began in the 1960's, it was not until 1992 when Unocal drilled Matalibong-25 as a slim hole for pressure monitoring, that continuous core from the reservoir became available for detailed studies. This well was drilled in the western part of the field where temperatures currently are close to 270°C (Fig. 1). Core was taken from 789 to 2439 m with 95% recovery. Various aspects of the fracture characteristics, lithologies, and wallrock alteration have been described by Nielson et al. (1995). In this paper, we present information on the hydrothermal mineralogy of the veins encountered in the cored section of the well and on fluid-inclusion temperatures, salinities, and gas contents of vein minerals. The data

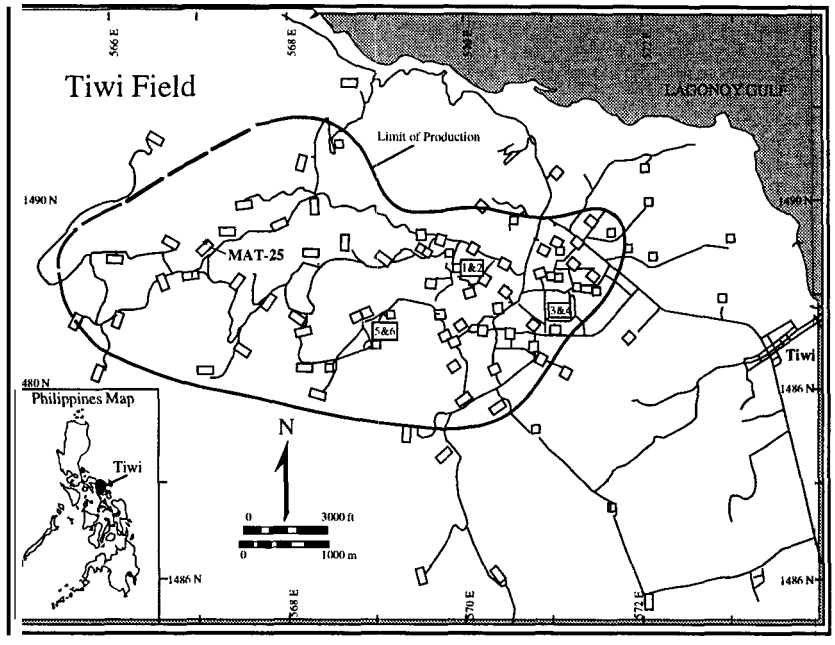

Figure 1. Map of the Tiwi geothermal field showing the location of roads and well pads. Numbered boxes are power plants.

are used to develop a picture of the thermal and chemical evolution of the rocks penetrated in Matalibong-25.

REGIONAL GEOLOGY

The Tiwi geothermal field is located on the northeastern flank of Mt. Malinao in southern Luzon, approximately 300 km from Manila. Mt. Malinao is an eroded volcano that was active between 0.5 and 0.06 Ma (Gambill and Beraquit, 1993). The reservoir is developed primarily in the volcanic rocks of Mt. Malinao and in the generally similar underlying rocks of the Miocene-Pliocene Polangui Volcanics. Beneath these reservoir rocks, the basement consists of sandstone, mudstone, and limestone that overlies quartz-muscovite schist. These metamorphic rocks have only been encountered in the eastern part of the field because of the westward thickening of the volcanic section.

The reservoir rocks are pervasively altered throughout the field (Gambill and Beraquit, 1993). Smectite and calcite are found along the top and sides of the reservoir while the interior is characterized by chlorite, quartz, and epidote. Pyrophyllite, alunite, anhydrite, and diaspore formed from high-temperature acidic fluids have been observed in the southwest and south-central parts of the field.

Figure 2 illustrates the lithologies encountered in Matalibong-25. The upper part of the well, above a depth of 1601 m, is dominated by andesite and basaltic andesite flows, flow breccias and volcaniclastic rocks deposited in a subaerial environment. Between 1601 and 2012 m, the appearance of poorly-sorted sandstones that are intercalated with claystones, andesite breccias, and lava flows mark the transition to a subaqueous environment. Below 2012 m, sandstone makes up more than 90% of the section.

METHODS AND PROCEDURES

FLUID-INCLUSION MICROTHERMOMETRY

Fluid-inclusion homogenization temperature and salinity measurements conducted as part of this study were made on doubly polished plates of quartz, calcite, and anhydrite using a Fluid Inc.-adapted USGS-type heating/freezing system calibrated with synthetic fluid inclusions. The accuracy of the microthermometric measurements, based on repeated measurements of the synthetic fluid inclusions, is estimated to be ± 0.1°C at temperatures below 0.0°C and ± 3.0°C

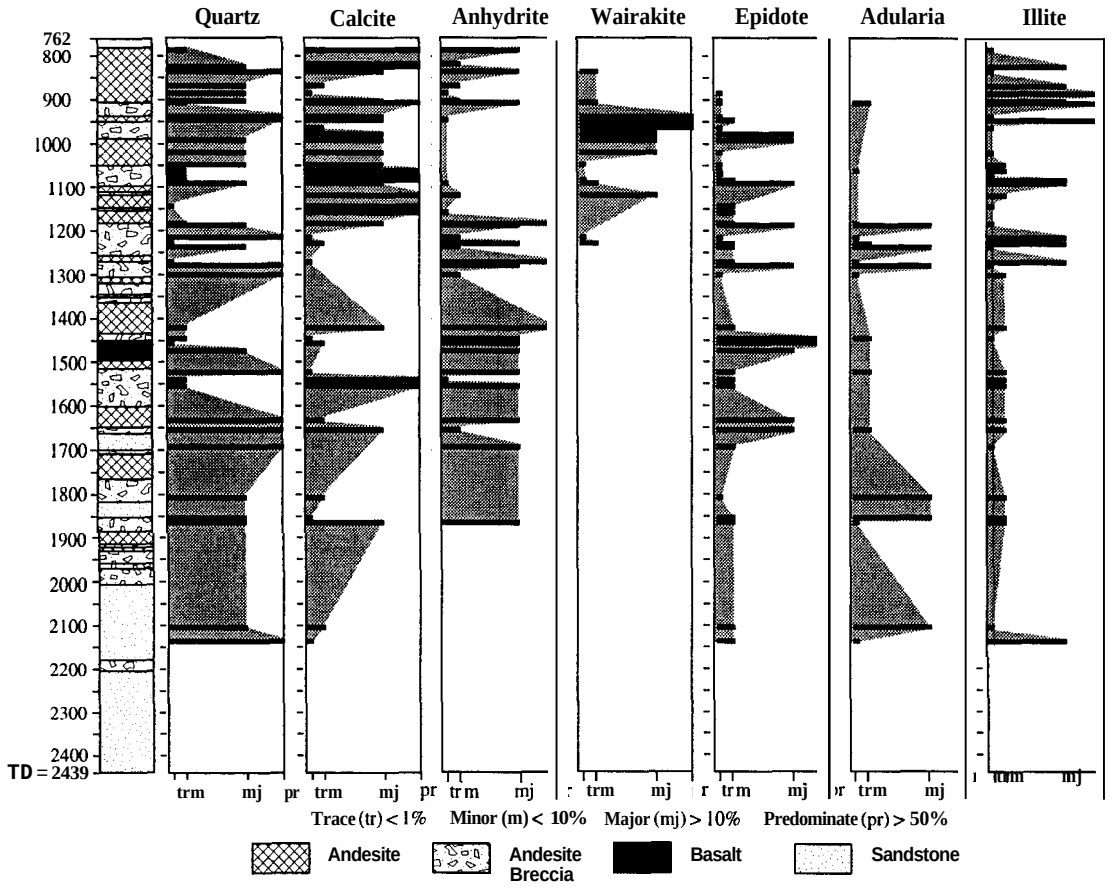

Figure 2. Lithologies and distribution of key alteration minerals in the cored portion of Matalibong-25.

at 375°C. The salinities of the inclusions were determined from ice-melting temperatures using the equation developed by Bodnar (1993).

FLUID-INCLUSION GAS CHEMISTRY

The gas compositions of the fluid inclusions were determined by quadrapole mass spectrometry after being liberated by crushing in a vacuum. Samples were analyzed for a variety of gases including Ar, H_2, He, CO_2, CH_4, C_{2-7}, H_2O, H_2S, N_2, O_2, and SO_2. Details of the methodology are described by Norman and Sawkins (1987) and Norman et al. (1996). In general, the precision of the analyses is estimated to be 10 to 20%.

HYDROTHERMAL ALTERATION OF MATALIBONG-25

Rocks in Matalibong-25 generally display moderate to strong hydrothermal alteration, particularly in the vicinity of the veins. From the top of the core to depths of 908 m, the wall rocks are characterized by sericite, calcite, chlorite, quartz, anhydrite, sphene, and pyrite. Within this zone, sericite is the dominant secondary phase. At greater depths, epidote joins the assemblage and remains a minor phase to depths of 1900 m when its abundance increases. Throughout most of the well, carbonate, chlorite, and sericite are the dominant phases. Although fluid-inclusion measurements demonstrate that temperatures reached or exceeded 300°C throughout most of the cored section of the well, minerals typical of these high-temperature conditions (e.g. garnet, biotite, pyroxenes) are uncommon, and only sporadic occurrences of actinolite were found in the veins.

Approximately 50 vein-bearing samples were petrographically studied between depths of 793 and 2135 m.

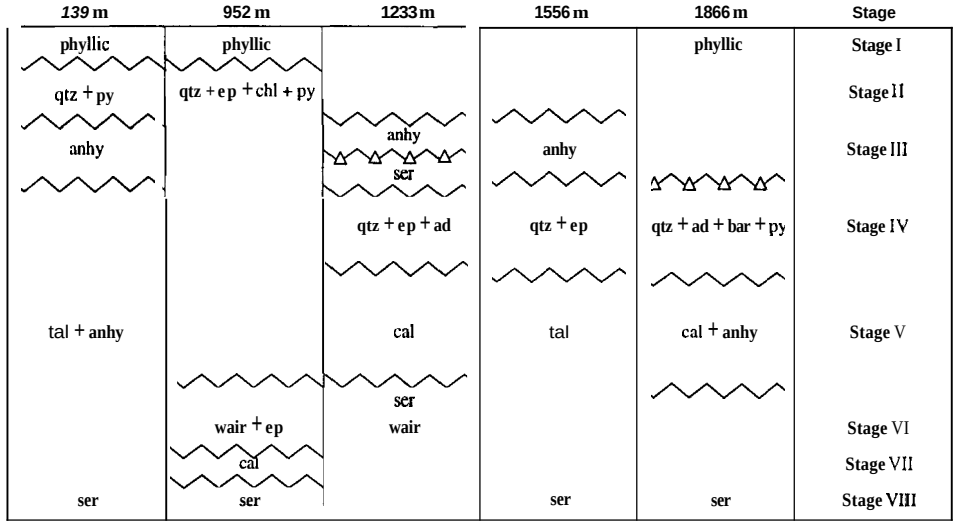

Figure **3.** Representative paragenetic sequences in selected samples. The zig-zag line indicates fracturing; triangles denote hydrothermal brecciation. Abbreviations: ad = adularia; anhy = anhydrite; bar = barite; cal = calcite; chl = chlorite; ep = epidote; qtz = quartz; ser = sericite; wair = wairakite. Numbers at the tops of the columns denote sample depths. The stage of mineralization is shown on the far right.

The vein minerals and their abundances are summarized in Figure **2.** Although the major vein minerals are generally similar throughout the well, there are systematic variations in the mineral abundances and distribution of minor phases. Four zones can be defined on the basis of these mineral distributions. Zone 1 extends from the top of the core to a depth of **831** m and is characterized by the presence of veins containing variable proportions of calcite, which is the dominant phase, quartz, anhydrite, and illite. Zone **2** extends from **831** to **1123** m. Within this zone, wairakite and epidote are both present, with wairakite being the dominant calcsilicate mineral. Zone 3 veins contain abundant anhydrite, epidote, and adularia. Calcite is important mainly at the top and bottom of the zone and wairakite is rare. Zone **3** extends from **1123** to **1657** m. The lowermost zone, zone **4,** extends from **1657** m to the bottom of the core. The presence of minor to trace amounts of barite, sphalerite, and galena are diagnostic of this zone. Adularia, epidote, anhydrite, and calcite persist. Quartz, illite, chlorite, pyrite, and sphene are present in all zones.

Eight stages of alteration and vein mineralization have been recognized on the basis of crosscutting relationships (Fig. 3). The earliest stage (stage **1)** appears to be represented by phyllic alteration of the volcanic rocks. Quartz displaying chalcedonic textures is present as vein and amygdule fillings at several depths (e.g. **831; 2437** m) and may also be related to this phase of mineralization. Stages **2** to **8** are represented by vein mineralization. Stage **2** veins are characterized by quartz + pyrite + epidote. The wallrocks associated with these veins are commonly silicified. Stage **3** veins are dominated by blocky, often coarse-grained anhydrite. In some samples the anhydrite is brecciated, while in others, the veins contain fragments of brecciated country rock. Rhombohedral calcite may be present but it is a minor phase in most veins assigned to this stage. Stage **3** veins are crosscut by veins dominated by epidote or quartz + adularia (stage **4)** although all three minerals may occur in the same vein. Veins deposited during stage **4** are the most diverse, with mineral abundances varying markedly even among individual fractures in the same thin section. Rarely, veins assigned to this stage consist of quartz and bladed calcite **(841** and **1052** m). Stage **5** veins are characterized by rhombohedral calcite and minor anhydrite. In addition, we include within this stage vug-filling calcite and anhydrite present in stage **4** veins and calcite that replaces adularia at **2105** m. Stage **6** mineralization is found only in the upper part of the well and includes veins of wairakite + epidote + quartz. The replacement of preexisting

calcite and anhydrite by epidote is common in this stage. Stage 7 mineralization is represented by calcite that fills open spaces in wairakite veins. The final stage of mineralization (stage 8) is characterized by illite ± chlorite. The occurrence of these minerals is important because they suggest a significant change in the chemistry of the mineralizing fluids. The sericite occurs in veins and as fine-grained irregular masses associated with corroded calcite and anhydrite or as radiating aggregates coating silicate minerals. Although sericite is typically the last mineral to have been deposited, in some samples multiple stages of late-stage sericite are present. Where present, this sericite invariably postdates stage 5 calcite and precedes stage 6 wairakite. We have arbitrarily assigned the late sericite in the lower part of the well to stage 7, rather than a pre-stage 6 event, because thermochemical modeling suggests that sericite is in equilibrium with the present fluids (Bruton et al., 1997).

Although actinolite is not common, it is an important index mineral because it is stable only above temperatures of 300°C (Henley and Ellis, 1983). Actinolite-bearing veins were found at 996, 1276, and 2135 m. In each case, actinolite occupies a different position in the paragenetic sequence. At the shallowest depth, actinolite postdates stage 6 wairakite and epidote and even later vug-filling calcite (stage 7) whereas at 1276 m, actinolite was deposited after stage 5 calcite but before younger anhydrite and sericite. At 2135 m, it appears to be contemporaneous with stage 4 veins containing quartz, epidote, and adularia.

RESULTS

FLUID-INCLUSION TEMPERATURES AND SALINITIES

More than 700 fluid inclusions were measured in vein calcite, quartz, and anhydrite from Matalibong-25. The vast majority of the inclusions we studied were secondary in origin, defining short, healed fractures within the crystal interiors. Rarely, as at 1866 m, the secondary planes occurred within a growth zone.

Only two-phase inclusions containing liquid and vapor at room temperature were observed in the samples. Although measurements were made only on liquid-rich inclusions, a significant proportion of the inclusions were found to contain more than 95% vapor. The presence of vapor-rich inclusions provides clear, independent evidence that boiling occurred throughout the cored portion of Matalibong-25.

The results of the fluid-inclusion measurements are shown in Figures **4** and 5 along with downhole measured temperatures, and the boiling-point curve for a 2.0 weight percent NaCl solution. Homogenization temperatures of the inclusions ranged from 366" to 191°C while salinities varied from 3.7 to 0.0 weight percent NaCl equivalent. Figure 4 shows that in general, the maximum temperatures closely follow the boiling point to depth curve. In contrast, the minimum temperatures show little relationship to depth. Temperatures below about 1524 m are nearly constant at 230°C; those at shallower depths are distinctly higher, ranging from about 250" to 260°C.

Figure 5 indicates that the maximum salinities of the fluid inclusions generally increase with depth. Below depths of 1600 m, the maximum salinities ranged from approximately 3.1 to 3.7 weight percent NaCl equivalent. These salinities are close to or slightly greater than that of seawater. In contrast, fluid inclusions from shallower depths have salinities that do not exceed 1.7 weight percent NaCl equivalent. For comparison, the composition of the reservoir fluid produced by Matalibong-25 yields an ice-melting temperature of -0.55°C which corresponds to a salinity of 1.0 weight percent NaCl equivalent.

FLUID-INCLUSION GAS COMPOSITIONS

The gas compositions of fluid inclusions in 15 samples of vein calcite, quartz, and anhydrite from depths ranging from 1113 to 2428 m were measured. The principal component of the inclusions was water, which accounted for 70 to 99.8 mole percent of the analyses. CO_2, CH_4, H_2, N_2, Ar, H_2S, SO_2, and hydrocarbons (C_{2-7}) were also detected in samples, with C02 and CH_4 dominating.

Figure 6 displays the concentrations of CO_2, CH_4, and N_2/Ar ratios of the samples with respect to depth. Most depths are characterized by relatively broad but similar ranges of compositions. The highest CO_2 and gas contents are found in the shallowest sample (915 m) while smaller enrichments in CO_2, up to about 5 mole percent, characterize samples from 1849 to 2123 m. In contrast, the highest concentrations of CH_4 are found between 1333 and 1849 m. N_2/Ar ratios ranged from 0 to 4701. Inclusions from 1849 m, yielded the highest N_2/Ar ratios and CH_4 contents.

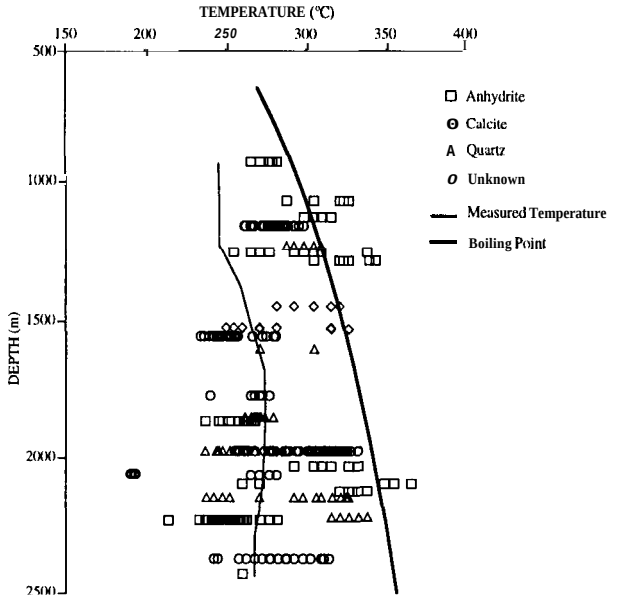

Figure 4. Distribution of fluid-inclusion homogenization temperatures in vein minerals as a function of depth. Data are from this study and from an unpublished Unocal investigation. For comparison, the measured temperatures and the boiling-point curve for a 2.0 weight percent NaCl solution are also shown.

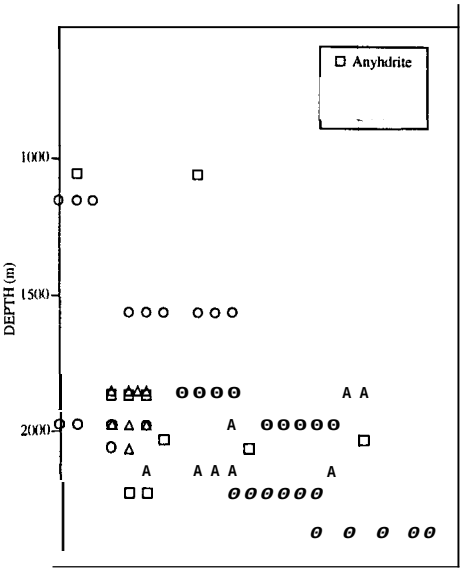

Figure 5. Distribution of fluid-inclusion salinities in vein minerals as a function of depth. Salinities are in weight percent NaCl equivalent Data sources are the same as those for Figure 4.

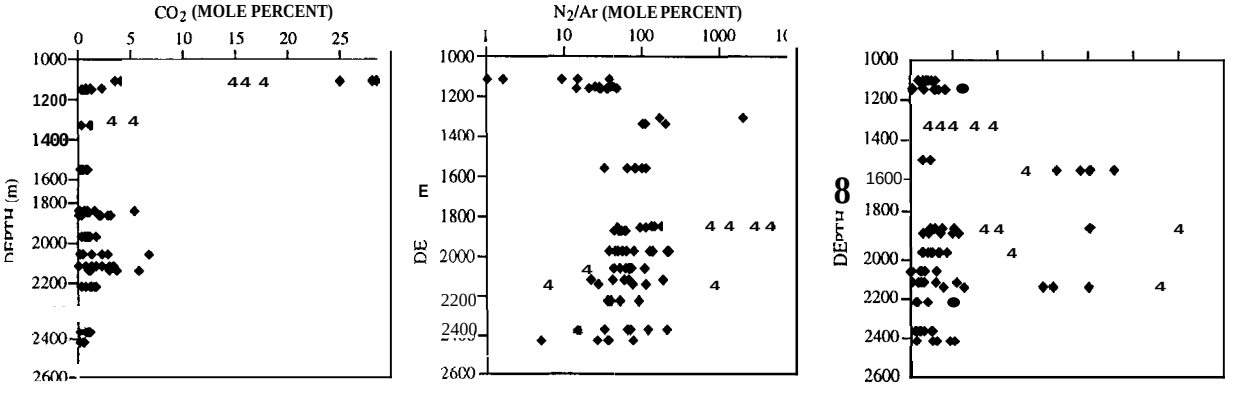

Figure 6. Distribution of CO_2, N_2/Ar, and CH_4 in fluid inclusions.

DISCUSSION

Mineralogic and fluid-inclusion data from Matalibong-25 provide a rare glimpse into the evolution of a long-lived geothermal system. We have recognized eight distinct stages of mineralization. The earliest stage appears to be represented by phyllic alteration of the volcanic rocks. No fluid inclusion data has been obtained on minerals deposited during this event. However, the deposition of chalcedony rather than quartz, which typifies the later stages of mineralization, suggests that temperatures may not have exceeded 180°C (Fournier, 1985). The distribution of vein assemblages and the mineral textures demonstrate that stages 2 through 8 formed under a variety of conditions and flow regimes. Stage 2 min-

erals (quartz, pyrite, and epidote) are indicative of boiling (Bruton et al., 1997). The anhydrite veins of stage 3 are monomineralic or contain minor calcite. The simple mineralogies of these veins, and the retrograde solubilities of both minerals suggests that they were deposited in response to heating of the thermal waters. Stage 4 mineralization is distinguished by the presence of adularia, open-space veins, and hydrothermal brecciation. These textures, and the deposition of adularia as open-space fillings in rocks containing illite suggest that boiling accompanied pressure release during fracturing (Browne and Ellis, 1970). Like stage 3 veins, stage 5 veins are mineralogically and texturally simple and consist of calcite or calcite + anhydrite. Crystals of calcite are typically blocky in habit, and the veins lack evidence of brecciation. These features contrast with its bladed habit and tendency to be intergrown with quartz in boiling zones, and imply deposition in response to heating. Stages 6 and 7, which is developed in the upper part of the well, suggest a renewed cycle of conductive cooling or boiling to produce wairakite and heating to deposit calcite (Bruton et al., 1997). Late-stage sericite (stage 8) and its common association with corroded calcite and anhydrite implies a change from neutral to slightly acidic conditions. An increase in the CO_2 content of the fluid related to deep boiling is the most likely cause of this pH change. Modeling by Bruton et al. (1997) suggests that sericite is in equilibrium with the present-day fluids.

Taken together, the vein parageneses document periods of upflow that oscillated with the incursion of cooler fluids during stages 3 (anhydrite dominant) 5, and 7 (calcite dominant). Fluid-inclusion temperatures in quartz, calcite, and anhydrite, however, show no systematic differences, and indicate that the maximum temperatures during stages 3, 4, and 5 remained at or near the boiling point and exceeded 300°C throughout most of the well (Fig. 4). Even though we were unable to obtain fluid-inclusion data on minerals clearly related to stages 2 and 6, the presence of epidote in these veins indicates that temperatures were above 240°C while post stage 7 actinolite at 996 m provides evidence of temperatures above 300°C (Henley and Ellis, 1983).

$^{40}Ar/^{39}Ar$ spectrum dating of adularia from a quartz-adularia-sulphide vein sampled at a depth of 1849 m indicates that the system has been active for more than 0.32 Ma (M. Hitzler, written comm. 1995). We have assigned this vein to stage 4 on the basis of its similarity to veins at 1866 m where younger calcite + anhydrite veins (stage 5) are also present. In addition, the spectra indicates that some leakage of Ar may have occurred between 0.32 and 0.25 Ma but since that time, temperatures have been no hotter than about 275°C. The occurrence of fluid inclusions with homogenization temperatures exceeding 300°C in calcite and anhydrite deposited during stages 3 and 5, and the presence of post stage 7 actinolite at 996 m, constrains the age of the main mineralizing stages (stages 2-7) to greater than 0.25 Ma.

Fluid inclusions from depths below 1524 m record cooling of the thermal system prior to development of the present thermal regime. Within this part of the well, minimum fluid-inclusion temperatures are generally similar and range from 225" to 250°C. The present-day downhole temperatures of approximately 270°C in the lower part of the well demonstrate renewed heating of the system, perhaps in response to the incursion of new magma beneath the field, Measured temperatures in the upper part of the well are substantially lower as a result of the production-induced development of a steam zone above 1219 m depth.

The salinities of the inclusion fluids demonstrate that two compositionally distinct waters were involved in the hydrothermal alteration. Veins formed below 1800 m contain fluid inclusions with apparent salinities close to seawater. In contrast, maximum salinities are less than 1.7 weight percent NaCl equivalent above 1829 m and there is an overall trend of decreasing salinity with decreasing depth. These observations imply that a lower salinity water dominates at shallow depths. Present-day pressure profiles are consistent with this observation and show that seawater pressures exceed reservoir pressures only below depths of approximately 1600 m while fresh groundwater pressures exceed reservoir pressures throughout the core depth. Thus, only fresh water can enter the reservoir above 1600 m. Below this depth, the inflow of both seawater and fresh water is possible.

Although the salinity data suggest that the inclusion fluids are dominantly mixtures of sea and meteoric water, few samples have N_2/Ar ratios typical of air-saturated water (approximately 36). Giggenbach (1986) showed that the gas compositions of geothermal fluids could be modified by interactions with

gases derived from magmatic and crustal sources and that the sources of the gases could be deduced from their relative abundances. In addition, significant variations in gas compositions can result from boiling (Norman et al., 1966, 1977). The addition of gases resulting from boiling can be easily recognized by high gas/water ratios in the fluid-inclusion data. Figure 6 shows that irrespective of the depth of trapping, most fluid-inclusion analyses yielded concentrations of C02 and CH4 that typically exceeded several mole percent. These gas concentrations are substantially higher than those in the present reservoir fluid. If it is assumed that only a single gas was present, Henry's Law constants at 270°C yield maximum gas concentrations of 0.6 to 2.6 mole percent for C02 and 0.2 to 1.1 mole percent for CH_4 at depths of 915 and 2439 m respectively (C. Bruton, pers. comm., 1996). We infer from these relationships that the fluid-inclusion data represent mixtures of vapor- and liquid-rich inclusions. Thus, the high gas contents of the inclusions provide independent evidence of boiling within the system. The highest gas contents are found at the shallowest depth. These gases appear to have been trapped beneath phyllically altered rocks that may form a low permeability cap over this part of the system.

The compositions of gases derived from magmatic and crustal sources are variable. Magmatic gases may contain CO_2, He, CO, H_2, SO_2, H_2S, N_2, and Ar and have N_2/Ar ratios that exceed 100 (Giggenbach, 1986). However, gases derived from crustal sources may also have elevated N_2/Ar ratios. Other gaseous species with crustal origins include CO_2, He, H_2S, CH_4, and hydrocarbons C_{2-7} (Norman et al., 1966). Figure 6 shows that most samples have N_2/Ar ratios ranging from air-saturated water (36) to 232. The excess N_2 in these samples suggests mixing between air-saturated water and a high N_2 source which in this case, may be either crustal rocks beneath the reservoir or a diluted magmatic fluid. In contrast, the extreme N_2/Ar ratios of inclusions from a depth of 1849 m suggest a possible magmatic origin. The high CH_4 contents are markedly different from the present-day fluids which are CH_4 poor. This argues that the fluid inclusions trapped gases generated during the early stages of the system's evolution.

CONCLUSIONS

The Tiwi hydrothermal system is developed in a thick sequence of Miocene to Pleistocene andesite and basalt flows, breccias, and volcanic sandstones that overlies a basement complex of marine deposits and mica schist. Detailed petrologic and fluid-inclusion studies have been conducted on Matalibong-25, which was drilled within the western part of the field where temperatures are presently close to 270°C. These studies, combined with $^{40}Ar/^{39}Ar$ dating document the development of a long lived hydrothermal system whose evolution can be divided into 3 major stages. The main features of these stages are summarized below.

INITIAL DEVELOPMENT OF THE TIWI SYSTEM

The early development of the field is represented by the presence of low- to moderate-temperature hydrothermal minerals within the reservoir rocks. In Matalibong-25, clays and chalcedony appear to be the earliest formed phases, occurring in veins and as vesicle fillings. Temperatures during this stage of alteration, based on the stabilities of these minerals probably did not greatly exceed 180°C (Fournier, 1985).

MAIN STAGE OF HYDROTHERMAL ALTERATION

A complex pattern of fluid circulation developed during the main stage of the system's evolution. Two major cycles, each consisting of a period of upwelling followed by recharge can be recognized in the mineral parageneses, although additional cycles are represented in individual samples. During the first cycle, the upwelling fluids produced quartz-pyrite veins and concurrent silicification of the adjacent wallrocks. This phase was followed by fracturing and the deposition of anhydrite veins that formed as fluids were drawn into the area and heated. The second cycle resulted in hydrothermal brecciation and the deposition of quartz, adularia and epidote followed by the deposition of calcite + anhydrite in newly developed fractures and as open-space fillings. $^{40}Ar/^{39}Ar$ dating of adularia indicates that this mineralization is at least 0.32 Ma and constrains the main stage of hydrothermal alteration to more the 0.25 Ma.

Thermodynamic modeling indicates that mineralization during the first half of each cycle resulted from boiling (Bruton et al., 1997). The incursion of cooler waters during the second phase of each cycle may have occurred in response to the development of pres-

sure sinks that formed as the fluids boiled off, causing the surrounding fractures to seal from mineral deposition. Despite the influx of these fluids, the maximum temperatures remained at or near the boiling point throughout these two cycles and exceeded 325°C at depths below 1970 m.

The hydrothermal fluids consisted of mixtures of fresh and seawater with seawater dominating at depths below about 1800m. Above this depth, the maximum salinities of the fluids decreased upward, indicating an increase in the proportion of fresh water. Gas ratios of fluid inclusions indicate the presence of a significant crustal component in the fluids at all depths.

THE PRESENT GEOTHERMAL SYSTEM

The present geothermal system represents a period of renewed heating that is probably related to emplacement of recent subvolcanic intrusions. Measured downhole temperatures have increased by approximately 35°C above the minimum fluid-inclusion temperatures, reaching a maximum of 270°C at about 1829 m. Below this depth, temperatures decrease slightly as the fracture intensity decreases (Nielson et al., 1996). This cooling and reheating has occurred within the last 0.25 Ma.

Thermodynamic modeling by Bruton et al. (1997) suggest that corrosion of calcite and anhydrite and the deposition of sericite as open space fillings may be modern features of the geothermal system related to recent boiling.

ACKNOWLEDGMENTS

This study would not have been possible without the support of the management and staff of the Philippine National Power Corporation, Philippine Geothermal, Inc., and Unocal Geothermal and Power Operations. We would like to thank D. Nielson for helping collect the samples, J. Hulen and C. Bruton for helpful discussions on the mineralogy of the well, and R. Turner and R. Wilson, who drafted the illustrations and helped put the paper together. Funding for JNM and GWJ was provided by the U.S. Department of Energy, under contract no. DE-AC07-951D 13274.

REFERENCES

Bodnar, R. J., 1993, Revised equation and table for determining the freezing point depression of H_2O-NaCl solutions: Geochemica Cosmochimica Acta, v. 57, p. 683-684.

Browne, P. R. L., and Ellis, A. J., 1970, The Ohaaki-Broadlands hydrothermal area, New Zealand: Mineralogy and related geochemistry: American Journal of Science: v. 269, p. 97-131.

Bruton, C. J., Moore, J. N., and Powell, T. S., 1997, Geochemical analysis of fluid-mineral relations in the Tiwi geothermal field, Philippines: Twenty-first Workshop on Geothermal Reservoir Engineering, Stanford University, in press.

Fournier, R. O., 1985, The behavior of silica in hydrothermal solutions *in* Geology and Geochemistry of Epithermal Systems (Berger, B. R., and Bethke, P. M., eds.): Reviews in Economic Geology, v. 2, p. 45-62.

Gambill, D. T. and Beraquit, D. B., 1993, Development history of the Tiwi geothermal field, Philippines: Geothermics, v. 22, p. 403-416.

Giggenbach, W. F., 1986, The use of gas chemistry in delineating the origin of fluids discharged over the Taupo Volcanic Zone: A review: International Volcanological Congress, Hamilton, New Zealand, Proceedings Symposium v .5, p. 47-50.

Henley, R. W., and Ellis, A. J., 1983, Geothermal systems ancient and modern: a geochemical review: Earth Science Reviews, v. 19, p. 1-50..

Nielson, D. L., Clemente, W. C., Moore, J. N., and Powell, T. S., 1996, Fracture Permeability of the Matalibong-25 Corehole, Tiwi geothermal system, Philippines: Twentieth Workshop on Geothermal Reservoir Engineering, Stanford University, p. 209-216.

Norman, D. I., and Sawkins, F. J., 1987, Analysis of gases in fluid inclusions by mass spectrometer: Chemical Geology, v. 61, p. 110-121.

Norman, D. I., Benton, L. D., and Albinson, T. F., 1991, Calculation of $f(O_2)$ and $f(S_2)$ of ore fluids, and pressure during mineralization from fluid inclusion gas analysis for the Fresnillo, Colorado, and Sombrerete Pb-An-Ag deposits, Mexico *in* Source, Transport, and Deposition of Metals (Pagel, M., ed.), Balkema Rotterdam, p. 468-476.

Norman D. I., Moore J. N., and Musgrave, J., 1997, Gaseous species as tracers in geothermal systems, Twenty-second Workshop on Geothermal Reservoir Engineering, Stanford University, in press.

Norman, D. I., Moore, J. N., Yonaka, B., and Musgrave, J., 1996, Gaseous species in fluid inclusions: a tracer of fluids and indicator of fluid processes: Twenty-first Workshop on Geothermal Reservoir Engineering, Stanford University, p. 233-240.